

Practical Use of Atomic-Scale Simulations for MYRRHA/XT-ADS Evolutionary and Innovative Nuclear Fuels

K. Govers, S.E. Lemehov, M. Verwerft, H. Aït Abderrahim

SCK•CEN, Boeretang 200, B-2400 Mol, Belgium

E-mail contact of main author: kgovers@sckcen.be

Abstract. The driver fuels today considered for MYRRHA, namely highly enriched (U,Pu)O₂ (MOX), can be considered as evolutionary fuels. The driver fuel will therefore largely rely on the experience gained from MOX deployment both in fast and thermal reactors. However, the foreseen migration of the core towards a facility for minor actinide transmutation will require novel concepts of fuel (inert matrix fuel bearing minor actinides: MgO, ZrO₂, Mo) which suffer from limited data in terms of in-pile behaviour and fall off the present validation range of empirical correlations still used in some of parts of fuel performance codes. Driven by similar needs for Gen-IV concepts, research presently evolves towards a fully mechanistic modelling of the fuel, based on a true description of the phenomena at play. The modelling of the driver fuel and the IMF targets for MYRRHA, as well as that of the present fuel, can also benefit from these efforts. In this paper, we will discuss the possible practical contribution of atomic-scale computer simulations in order to better understand and model different phenomena at play during the fission gas release process. We will show the progress made at SCK•CEN in terms of atomic-scale fuel modelling, by covering both atomic scale diffusion and irradiation effects (enhanced diffusion, trapping, re-resolution of intragranular bubbles. . .). These studies are conducted in the framework of the fuel R&D programme for Gen-IV & ADS systems at SCK•CEN.

1. Introduction

MYRRHA is conceived to be a pilot, experimental research reactor that must give a proof to the ADS concept and demonstrate the transmutation of higher actinides (americium and curium) in an effective way. It has a liquid Pb – Bi metal cooled fast neutron core fuelled with high-enriched (U,Pu)O₂ mixed oxide (MOX) fuel pins. Their better neutronic properties in a fast neutron spectrum over uranium dioxide and the large operational experience in the production and employment of MOX in Europe both for fast neutron reactors and for light water reactors made it the primary candidate as driver fuel. For demonstration of the viability of minor actinides transmutation, experimental fuel assemblies with fuel rods containing high concentrations of minor actinides will be loaded in MYRRHA's core.

In this context of the employment of well-known nuclear fuel – (U,Pu)O₂ – in a different environment (coolant, neutron spectrum, temperature) and with different design constraints (enrichment, Pu vector) and the envisaged use of fuels of a totally new concept (inert matrix fuels with high content of minor actinides), one is confronted with the endeavour to confirm one's understanding of the phenomena at play in nuclear fuel, and to predict the behaviour of unknown compounds showing a quite different behaviour. One approach to tackle this task, is the use of calculations at the atomic scale. Thanks to the computing power nowadays available, atomic scale calculations can provide insights on the primary processes governing mechanisms such as diffusion, clustering of impurities and amorphisation of crystalline structures. Not only the study of primary processes, but also physical quantities such as diffusion coefficients, melting point, can be derived from atomic scale calculations, which makes them a powerful tool in the assessment of novel

materials or the re-assessment of known materials in a novel environment. This paper will present some contributions of molecular dynamics studies on fission gas release processes and derived diffusion coefficients.

2. Description of the techniques

2.1. Interatomic potential

In the atomic scale simulation techniques considered at SCK•CEN, the level of empiricism is reduced to the accuracy in the description of atom interactions. Other techniques, very demanding in terms of computational resources, explicitly treat the electrons (ab initio calculations). They are commonly used as references for basic calculations with semi-empirical potentials, but are not used at the moment at SCK•CEN.

The basic idea behind empirical interatomic potentials is to approximate the configurational energy $V(\mathbf{r})$, where \mathbf{r} stands for the position of all atoms in the system, using “simple” analytical functions describing atoms interactions as a function of their positions only. One generally distinguishes between four types of bonding, which differ by the behaviour of the outer shell electrons [1]:

- Metallic bonding, in which delocalization of the electrons occurs;
- Covalent bonding, in which electrons are shared in a molecular state;
- Ionic bonding, with full transfer of electrons, resulting in electrostatic interaction;
- Weak chemical bonds, due to momentary dipole interactions of outer electron shells.

One of the simplest way to describe these interaction is to use pair potentials, which is very poor for metals or semi-conductors, but gives very good results for ionic compounds, since electrostatic forces are the dominating interactions.

Three types of interatomic potentials have mainly been used to describe interactions between uranium, oxygen and noble gases.

$$\text{Lennard-Jones potential: } V(r) = \frac{A}{r^{12}} - \frac{B}{r^6} \quad (1)$$

$$\text{Buckingham potential: } V(r) = A \exp\left(-\frac{r}{\rho}\right) - \frac{C}{r^6} \quad (2)$$

$$\text{Morse potential: } V(r) = D \{ [1 - \exp(\beta(r - r^*))]^2 - 1 \} \quad (3)$$

2.2. Simulation techniques

Keeping the simple picture of pair interactions, the interatomic potential energy as well as the interatomic forces are evaluated for all pairs of interacting atoms. In order to accelerate the simulation, the contribution of faraway pairs of atoms are neglected, by applying a certain cut-off to the computed interactions. Different techniques based on interatomic potentials have been considered:

- Energy Minimization (EM) calculations, in which atom positions are relaxed until an energy minimum is found. Such techniques are commonly used to derive defect energies – formation, migration (adding constraints), binding energies. . .
- Nudged Elastic Band (NEB) calculations, which simultaneously energy-minimize a set of intermediate configurations in order to find the migration energy as well as the migration pathway between two (known) atomic configurations.

- Molecular Dynamics (MD) techniques, in which one follows the time-evolution of the system. Forces acting on all atoms are calculated at regular intervals from the interatomic potential in order to determine their trajectories. Thermodynamic properties can then be derived thanks to statistical physics. Molecular dynamics also offer the possibility to study off-equilibrium processes, such as displacement cascades.

3. Achievements in terms of fission gas behaviour

3.1. Generalities

Different aspects of fission gas behaviour can be (and have been) studied with empirical potentials. The most straightforward properties are the energies related to these fission products: incorporation / solution energies, and the migration energy. Solution energies play a key role to determine the most stable configuration, i.e. the defect cluster occupied by fission gas atoms, as well as to determine their migration energy, since the formation of temporary cluster can assist their migration.

The diffusion coefficient itself can be investigated by following the time-evolution of the system, with MD techniques. They also offer the possibility of separate effect studies, by determining exactly the type and initial location of defects. Even more complex phenomena can be targeted, such as the interactions of noble gases with displacement cascades or (still more energetic) thermal spikes. It enables to understand the formation and destruction of intragranular bubbles which act as temporary traps for fission gases.

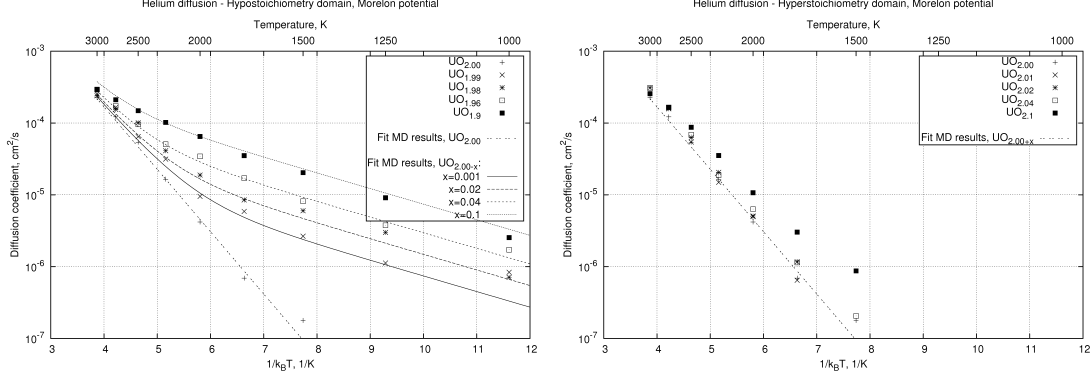
3.2. Helium behaviour in the lattice

Our study on helium mainly focused on its diffusion through the lattice. As mentioned, this process can be investigated with MD simulations. The following results have been obtained with the Morelon potential, coupled to the He interactions derived by Grimes [2]. A more detailed description of this work can be found in [3].

MD simulations of He in UO_2 were made at temperatures ranging from 1000 to 3000 K, by steps of 250 K. Various departures from stoichiometry were in each case considered in order to derive an Arrhénius expression for He diffusion in the different stoichiometry domains. The departure from stoichiometry was modelled by creating randomly dispersed oxygen point defects: vacancies and interstitials for respectively the hypo- and hyperstoichiometric regions.

The derived diffusion coefficient is illustrated in Fig. 1a. and 1b. (respectively the hypo- and hyperstoichiometry domains). It clearly appears on these graphs that He diffusion at low temperatures is assisted by oxygen vacancies, and presents a very low activation energy, around 0.5 eV. In the high temperature region, as well as for stoichiometric and hyperstoichiometric uranium dioxide, the activation energy presents a higher value, around 2.1 eV. Such a behaviour could be expected since at high temperature, or in absence of structural defects, thermally generated defects dominate whose concentration shows a Boltzmann dependance on both the temperature and the formation energy of the defect. In that case, the activation energy is given by the sum of the migration energy and the formation energy of the assisting defect. However, in that case, a still larger activation energy should be observed in the hyper-stoichiometric domain (since the formation energy of a vacancy in UO_{2+x} amounts to E_{OFP}), which is not the case. Therefore, the 2.1 eV activation energy should correspond to a second, intrinsic, migration mechanism. This interpretation has been confirmed by NEB calculations (see [3]), where it appeared that migration occurs through jumps of He atoms between octahedral interstitial positions.

FIG. 1.: He diffusion coefficient. Left: Hypostoichiometry region; Right: Hyperstoichiometry region



The expression that we could derive for He intrinsic diffusion coefficient (i.e. in UO_2 and UO_{2+x}) and for the V_O -assisted mechanism (in UO_{2-x}) are respectively:

$$D_{\text{He,int}} = 0.5 \exp\left(\frac{-2.0\text{eV}}{k_B T}\right) \text{cm}^2/\text{s} \quad (4)$$

$$D_{\text{He,V}_\text{O}} = 0.011 \cdot x \cdot \exp\left(\frac{-0.5\text{eV}}{k_B T}\right) \text{cm}^2/\text{s} \quad (5)$$

3.3. Xenon behaviour: attempt to determine the activation energy

In view of the small systems and timescales that can be considered in a reasonable amount of computing time, the simulation of the diffusion process by MD is limited to mechanisms presenting a low activation energy. Although advanced techniques, like Temperature Accelerated Dynamics (TAD) or Biased Potentials Dynamics (BPD), have been developed to partly circumvent this drawback of MD, Xenon migration (which usually presents high activation energies) has been investigated through static calculations. It was indeed necessary in view of the number of different cluster a Xe atom can be located in.

The relative energy of defect clusters govern the stable location of Xe atoms in the matrix as well as the defect configurations involved in Xe migration. These results are of key importance to understand the diffusion of single atoms in the matrix and subsequently to model Xe diffusion in fuel performance codes. Incorporation energies were found to be very high [4], because of the large size of Xe atoms, which explains the tendency for these atoms to precipitate as intra- or intergranular bubbles. Only one type of defect, the tetravacancy ($2\text{V}_\text{U} + 2\text{V}_\text{O}$) presented a much lower incorporation energy. Our investigations also showed that Xe migration mostly occurs in defects involving two uranium vacancies, with an energy barrier between 0.3 and 1.5 eV, well below the migration energy of uranium vacancies (2.4 – 3.0 eV in the bulk, ~ 3.5 eV in the different clusters). It confirmed the general hypothesis [5] that the migration of uranium vacancies is the rate-determining step for Xe diffusion. The migration barrier to interstitial sites was shown to be too high (more than 8 eV) in order to be an efficient mechanism.

The low incorporation energy in the tetravacancy, compared to other clusters, makes its formation energetically accessible. Based on the data obtained (see [4]), different migration mechanisms can be envisaged. They are summarized in Table I. The uncertainties, particularly on the oxygen Frenkel pairs and Schottky trios energies, impose to take this discussion with caution, since other mechanisms could be favored taking other values.

Hypostoichiometric fuel Trivacancies are the stable solution site, since oxygen vacancies are structurally available. Xe migration occurs through the formation of tetra-

TABLE I: ACTIVATION ENERGY FOR DIFFERENT MIGRATION MECHANISMS IN THE THREE STOICHIOMETRY DOMAINS WITH $E_{\text{OFP}}=3$ eV, $E_{\text{Sch}}=7$ eV.

	UO_{2-x}	UO_2	UO_{2+x}
<i>trap site</i>	Tri-vacancy	Tetra-vacancy	V_{U}
<i>defect for migration</i>	Tetra-vacancy	idem	–
<i>rate-determining step</i>	V_{U} migration in the defect	V_{U} migration in the defect	V_{U} migration <i>to</i> the defect
E_{mig}	3.5 eV	3.5 eV	2.4 eV
$\Delta E_{\text{form. const.}}$	$E_{V_{\text{U}}}=E_{\text{Sch}}$	0	$E_{V_{\text{U}}}=E_{\text{Sch}} - 2 E_{\text{OFP}}$
$\Delta E_{\text{binding}}$	~ -2 eV	0	–
$\Delta E_{\text{Xe incorporation}}$	~ -2.5 eV	0	–
E^*	~ 6.0 eV	3.5 eV	~ 2.4 eV
Experimental E^*	6.0 eV	3.9 eV	1.7 eV

vacancies, and the combined migration of the Xe atom together with the tetravacancy. The activation energies determined agree with the experimental tendency of 6.0 eV in UO_{2-x} [6].

Stoichiometric fuel Different solution sites have a similar (less than 1 eV difference) formation energy and could be envisaged : di-, tri- and tetra-vacancies. The uncertainties on the different parameters do not allow to select the most stable one, but neglecting the difference in binding energy, the activation energy can be approximated by the migration energy of a uranium vacancy *in* the cluster. Here again, this value is in good agreement with the experimental one, 3.9 eV [6]

Hyperstoichiometric fuel Xe is preferentially located in single uranium vacancies. Different migration mechanism can be envisaged, accounting for the fact that the creation of oxygen vacancies is difficult. The first one is again the migration of tetravacancies and the Xe they contain, a second mechanism could be via a $V_{\text{O}} + 2 V_{\text{U}}$ defect instead, or, finally, in view of the very low experimental activation energy (1.7 eV [6]) a simple uranium-vacancy assisted mechanism. It provides indeed the lowest activation energy, that of uranium vacancy migration : between 2.5 and 3.5 eV according to static calculations (2.4 eV were obtained by MD in [4], a similar value is obtained experimentally). Experimental determination of Xe diffusion coefficient shows a slightly lower activation energy than uranium vacancies, with 1.7 eV.

4. Predictive aspects of MD: insight on thermal spikes

4.1. Generalities on irradiation damage

Once the potentials have been validated against experimental data on known processes [3, 4, 7, 8], one can go one step further and start investigating phenomena that are not accessible to experiment. An important field where atomic-scale simulations can play a major role is the understanding of irradiation damages. Displacement cascade that reproduce the collision chain initiated by a primary knock-on atom (PKA) are now simulated for more than one decade in different kind of materials: metallic systems; glasses; ionic compounds, including uranium dioxide [9, 10]. An increase of the energy of the PKA implies in an increase of the system size (to include the whole recoil length and to dissipate the energy) and a decrease of the timestep (to keep a reasonable atomic displacement over each timestep). Nowadays limit in uranium dioxide is around 100 keV for the PKA. Moreover, in the higher energy range, other phenomena come at play, such as the electronic stopping power. Such effects are not covered by conventional MD.

Irradiation damage caused by swift ions has been modelled for a long time using the thermal spike (or ion track) model, in order to describe dust formation in interstellar space [11], or as a concept to describe the destruction of gas bubbles in nuclear fuel [12–14]. The local disorder created in the wake of swift ion trajectories, comes from direct interactions with the fission fragment, as well as from secondary collision cascades and dissipation of electronic excitations. The deposited energy will rapidly spread over a large amount of atoms along the fission fragment pathway: the thermal spike.

4.2. Methodology

This simple description can also be implemented for molecular dynamics simulations [4, 15, 16]: a cylindrical zone is selected where atoms were initially given a higher kinetic energy, typically a few eV per atom. After less than 100 fs the melting of this zone occurs, reproducing the idealized picture of the thermal spike. Electronic excitations, due to electronic stopping power, are not intrinsically taken into account in this approach, even though it could be partly accounted for by increasing the local energy. Neither is energy deposit at larger distance from the thermal spike core, due e.g. to very energetic PKA's. Some phenomena occurring during the cooling down phase are also neglected with this approach, like the electronic component for thermal conductivity, emission of photons etc. Only the ionic component (phonons) of thermal conductivity is intrinsically handled, but it seems sufficient to gain some information on the thermal spike duration, its diameter, and the defects that will be created.

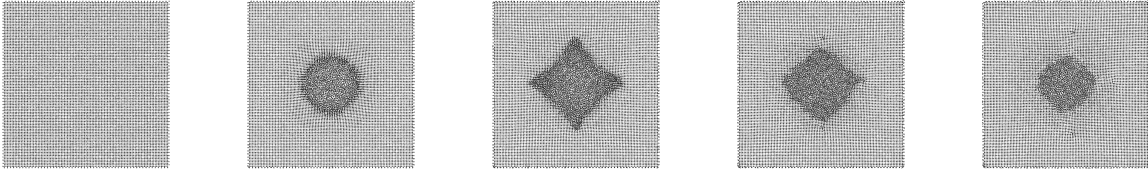
In order to reduce the computing needs, it is possible to only consider one slab and assume periodicity/symmetry along the spike, considering the long recoil length ($\sim 6 \mu\text{m}$) compared to the typical diameter (the order of 10 nm) of thermal spikes. A certain thickness was, however, still required for the slab in order to avoid artifices due to the periodic boundary conditions.

4.3. MD simulations of thermal spikes

In our simulations of thermal spikes, atoms at a distance below 3 nm were given a velocity which correspond to an average kinetic energy of 3 – 4 eV/atom. It simulates an energy deposit of 4 – 8 keV/nm, which is typical of the nuclear stopping power of energetic ions in UO_2 . Different parametric studies have been performed to better characterize the event: size of the simulation box, energy deposit, radius of the initial cylindrical zone and thermostatting at the border. Snapshots of the thermal spike evolution are shown in Fig. 2, the full animation is available as a separate file. The time before complete re-solidification of the system ranges between 60 and 80 ps. The thermal spike axis considered was the $\langle 100 \rangle$ direction. Other orientations will be considered in subsequent work.

The first stage of the thermal spike consists of the melting of the inner zone and the emission of energetic shock-waves, which can take about one fifth of the energy away from the thermal spike core. The damping of these shock-waves at the border of the simulation box has to be efficient in order to avoid their come-back to the central zone (reflexion on free surfaces or interaction with the images in case of periodic boundary conditions). The efficiency of the damping was assessed by varying the thermostatting parameter at the border. The re-scaling procedure seemed unefficient for damping since the velocity direction is not modified. A better choice seems to re-initialise atom velocities over the outer 2 – 3 nm every 200 – 500 fs. This choice permits the shock-wave to enter the border zone and to be damped there. Short re-initialisation intervals showed in a

FIG. 2. Snapshots of the thermal spike evolution, at 0, 1, 5, 12 and 30 ps.



reflexion of the shock-wave on the inner size of the border zone, resulting in a less efficient thermostating.

After this stage, the liquid zone expands. Oscillations of the liquid density are at the same time observed. An interesting point is that the liquid zone propagates slower in the $\langle 110 \rangle$ direction, leading to the formation of a square section whose sides are in $\langle 110 \rangle$ directions. The parametric studies on box size and thermal spike characteristics (radius and energy deposit) confirmed the interpretation relative to the square form. Therefore, it cannot be attributed to artifices due to shock-wave reflection. The maximal diameter observed, for an initial energy deposit of 6 keV/nm, is around 10 nm.

Then solidification of the melt starts. During this process, misalignments were observed, leading to the apparition of dislocation loops. Dislocations were not created during all simulations, it seems that a certain threshold of energy deposit needs to be reached before their apparition, the range being 5 to 7 keV/nm. No amorphisation of the uranium dioxide matrix has been observed.

The extension of this work to interactions with fission gas bubbles is still under progress. Such results would enable the determination of the re-resolution parameter.

5. Issues and perspectives

The present paper provided an overview of the present research at SCK•CEN in terms of fission gases behaviour at the atomic scale. These results are of key importance to determine the effective diffusion coefficient commonly used in fuel performance codes which governs the macroscopic release rate and includes trapping and re-resolution effects, grain growth, bubble coalescence etc.

More generally, the paper attempted at showing the possible contribution of MD techniques to better understand and model the present and future nuclear fuels by focusing on some aspects of fission gases behaviour. However, this choice is not limiting and other aspects of fission gas release, as well as different phenomena could have been tackled. One can think for example about modelling point and extended (precipitates, dislocations, grain boundaries) defects; the assessment of defects influence on thermal conductivity; investigation of the high burnup structure; etc. These results are meant to be used in a later stage in mechanistic fuel performance codes.

The present research is still performed on uranium dioxide, in view of its wide use as reference material in experiments and of the lack of experimental data on other fuel types. It is only once confidence has been reached for modelling UO_2 that the extension of such computational work to evolutive (MOX) or novel types (IMF targets CERMET and CERCER) of fuels can trustfully commence.

Acknowledgments

This paper summarized past studies made at SCK•CEN as well as present and future work which are funded by the F-Bridge and Fairfuels European program (EFP7). Within F-Bridge, the authors wish to underline the collaboration with L. van Brutzel (CEA, France) to characterize the thermal spikes.

References

- [1] R. Tilley, *Understanding solids*, Wiley, 2004.
- [2] R. Grimes, R. Miller, C. Catlow, The behaviour of He in UO_2 : solution and migration energies, *J. Nucl. Mater.* 172 (1990) 123.
- [3] K. Govers, S. Lemehov, M. Hou, M. Verwerft, Molecular dynamics simulation of He diffusion in UO_2 , Submitted to *J. Nucl. Mater.*
- [4] K. Govers, Atomic-scale simulations of noble gases behaviour in uranium dioxide, Ph.D. thesis, Université Libre de Bruxelles (ULB), Belgium (2008).
- [5] H. Matzke, Diffusion processes and surface effects in non stoichiometric nuclear fuel oxides UO_{2+x} and $(\text{U,Pu})\text{O}_{2\pm x}$, *J. Nucl. Mater.* 114 (1983) 121.
- [6] W. Miekeley, F. Felix, *J. Nucl. Mater.* 42 (1972) 297.
- [7] K. Govers, S. Lemehov, M. Hou, M. Verwerft, Comparison of interatomic potentials for UO_2 Part I : Static calculations, *J. Nucl. Mater.* 366 (2007) 161.
- [8] K. Govers, S. Lemehov, M. Hou, M. Verwerft, Comparison of interatomic potentials for UO_2 Part II : Molecular dynamics simulations, *J. Nucl. Mater.* 378 (2008) 66.
- [9] L. Van Brutzel, M. Rarivomanantsoa, Molecular dynamics simulation study of primary damage in UO_2 produced by cascade overlaps, *J. Nucl. Mater.* 358 (2006) 209.
- [10] D. Parfitt, R. Grimes, Predicted mechanisms for radiation enhanced helium resolution in uranium dioxide, *J. Nucl. Mater.* 381 (2008) 216.
- [11] R. Devanathan, P. Durham, J. Du, L. Corrales, E. Bringa, Molecular dynamics simulation of amorphisation in forsterite by cosmic rays, *Nucl. Instr. Meth. Phys. Res. Sect. B* 255 (2007) 172.
- [12] H. Matzke, Gas release mechanisms in UO_2 : a critical review, *Rad. Eff.* 53 (1980) 219.
- [13] J. Turnbull, C. Friskney, J. Findlay, F. Johnson, A. Walter, The diffusion coefficients of gaseous and volatile species during the irradiation of uranium dioxide, *J. Nucl. Mater.* 107 (1982) 168.
- [14] M. Speight., , *Nucl. Sci. Eng.* 37 (1969) 180.
- [15] O. Tucker, D. Ivanov, L. Zhigilei, R. Johnson, E. Bringa, Molecular dynamics simulation of sputtering from a cylindrical track : Eam versus pair potentials, *Nucl. Instrum. and Meth. in Phys. Res. Sect. B : Beam Interact. with Mater. and Atoms* 228 (2005) 163.
- [16] D. Young, Molecular dynamics simulation of swift ion damage in lithium fluoride, *Nucl. Instr. Meth. Phys. Res. Sect. B* 225 (2004) 231.